ISSN 1392–1320 MATERIALS SCIENCE (MEDŽIAGOTYRA). Vol. 19, No. 4. 2013

Improvement of Tribological Properties of Metal Matrix Composites by Means of Slide Burnishing

Piotr BEDNARSKI [1], Dionizy BIAŁO [2], Witold BROSTOW [3 *], Kazimierz CZECHOWSKI [1], Waldemar POLOWSKI [1], Piotr RUSEK [1], Daniel TOBOŁA [1]

[1] *Institute of Advanced Manufacturing Technology (IAMT), Wrocławska 37a, 30-011 Cracow, Poland*
[2] *College of Mechatronics, Warsaw University of Technology, Boboli 8, 02-525 Warsaw, Poland*
[3] *Laboratory of Advanced Polymers & Optimized Materials (LAPOM), Department of Materials Science and Engineering, Department of Physics and Center for Advanced Research and Technology (CART), University of North Texas, 3940 North Elm Street, Denton, TX 76207, USA*

crossref http://dx.doi.org/10.5755/j01.ms.19.4.2404

Received 06 September 2012; accepted 13 January 2013

Burnishing of metal surfaces can affect positively tribological and mechanical properties such as fatigue strength, wear resistance, contact stiffness and bearing capacity. Burnishing affects the entire surface topography, including surface roughness, radii of curvature of peaks and valleys, slope angles and more. We have studied A1Mg1SiCu (6xxx series) aluminum matrix composites with a reinforcing phase of Al_2O_3 which exhibits good workability but poor machinability. The second series studied was based on an AlSi alloy (A-390) reinforced with SiC – this one characterized by poor workability but good machinability. Materials have been prepared by mixing metal powders with the reinforcement, cold pressing, sintering, hot extrusion and heat treatment. We have determined surface roughness with a Hommel tester; the arithmetical mean for A1Mg1SiCu (A6061 + Al_2O_3) was ~1 μm before burnishing and ~0.15 μm after burnishing. We have also determined the bearing capacity at 50 % with the same tester: before burnishing 2.30 μm and 0.47 μm afterwards for A6061 + Al_2O_3; before 2.30 μm, afterwards 0.37 μm for A390 + SiC. Vickers microhardness at the surface with respect to the core increases 30 % for the Al_2O_3 containing composite and 50 % for the SiC containing composite.
Keywords: metal matrix composites, slide diamond burnishing, surface roughness.

1. INTRODUCTION

Burnishing of metals is a relatively easy way to improve properties of components, especially in aerospace and automotive industries. The cost of process is not high because most of burnishing tools are very reliable and durable and the equipment to be used does not require additional reconstruction. Expected results of burnishing include improvement of tribological and mechanical properties without a modification of design or any other modification of the technology. More generally, in multiphase systems the surfaces and interfaces largely determine the properties [1, 2].

Originally the burnishing process was introduced to the railway axles approximately a century ago. Further developments resulted in more than 20 different specific procedures adapted to a variety of parts for a variety of industries. As expected, improved knowledge of the process has resulted in its better control and repeatability.

However, there is a room for still further improvement. New materials, including metals with low density are coming on board. This applies also to metal matrix composites (MMCs) now used more and more in the engineering practice.

New tools design and new tool materials have also broadened the field of potential applications of the burnishing process [3, 4].

*Corresponding author. Tel.: +1-940-565-4358, fax: +1-940-565-4824, E-mail address: *wbrostow@yahoo.com* (W. Brostow)

2. MOTIVATION AND CHOICE OF COMPOSITES

There are good reasons to investigate slide burnishing [5, 6] as the finishing process for many MMCs composites. We need to understand better how burnishing changes the whole surface topography, strengthens the surface and affects the properties of the products.

Burnished surfaces have been reported to resist high dynamic loads and pressures, exhibit low friction and low wear, thus providing longer service life and more reliability to the machine elements [7]. Physical phenomena of the process consists of elastic and plastic strains, internal compressive stresses formation which enlarge the energy of the crystal lattice and increases the hardness of the surface layer [8, 9]. Thermal effects do not affect the properties of the upper layer because of a small volume of material undergoing deformation and moderate process conditions in terms of speed, feed and the pressure applied. Moreover, spray lubrication is used to take away a large part of the frictional heat created from the tool – workpiece contact.

A burnishing tool easily deforms the surface – even a very hard one – because of a small tool – workpiece contact area. Burnishing can improve dimensional accuracy when a stiff burnishing tool (burnisher) is used. Important for the properties of the final products are surface geometry improvements [10, 11].

There are also hybrid processes such as electro chemical machining (ECM) burnishing [12], laser – burnishing [13, 14], electro discharge machining (EDM) burnishing [15] and shot peening – burnishing [11].

The burnishing processes by no means bring about automatic improvement of mechanical or tribological properties. This applies to MMCs in particular; information on their performance under service conditions is still limited.

Towards this end we have studied two metal matrix composites. We have applied burnishing to wrought A6061 + Al_2O_3 (covered by the ANSI standard H35.1) and to AlMg1SiCu + Al_2O_3 (covered by an ISO standard) composite as the final finishing process. The matrix base of A6061 consists of 0.4 % – 0.8 % Si, 0.7 % Fe, 0.15 % – 0.4 % Cu, 0.8 % – 1.2 % Mg, 0.15 % Mn, the remainder being Al [16]. Bars with the diameter ∅ = 35 mm were hot extruded and air cooled. Sintering and extrusion conditions defined by P/M Laboratory, Delft, were followed [17].

Main applications of A6061 involve heavy duty structures requiring good corrosion resistance: aircraft, truck and marine, railroad cars, furniture pipelines [18]. Unfortunately A6061 does not resist abrasive environments and has poor contact wear resistance. Adding Al_2O_3 to the matrix material was expected to improve wear performance. We have applied 15 wt.% of 17 μm Al_2O_3 particles [19].

The second composite studied was as cast A390 + SiC. The base material contains 4 % – 5 % Cu, 0.45 % – 0.65 % Mg, 16 % – 18 % Si, 0.5 % Fe max, 0.1 % Mn max. [10]. Applications of the A390 include automotive cylinder blocks, four cycle air-cooled engines, air and cooling liquid compressors, pumps requiring abrasive resistance, pulleys and brake shoes, and also other applications where high wear resistance, low thermal expansivity and/or good elevated temperature strength are required. In this case 2.5 % of 7 μm diameter SiC particles were added [19, 20].

Our MMCs – A6061 + Al_2O_3 composite exhibits good workability – but relatively poor machinability – while A390 + SiC exhibits just the opposite behavior.

3. EXPERIMENTAL

We have used diamond burnishers of DCB (diamond composite burnisher) type produced in IAMT, with the tips made of a synthetic diamond in the shape of spherical caps with the radius R = 3.5 mm.

A synthetic diamond was composed of diamond grains and a ceramic bonding phase, namely titanium silicon carbide Ti_3SiC_2. Literature reports tell us that this bonding phase can impart high temperature resistance, chemical resistance, rigidity, improved abrasive wear resistance and low friction on metal surfaces [2, 21 – 24]. The composite does not contain graphite – what was expected to have a beneficial effect on its mechanical properties.

The aim of our work was determination of the possibilities of using diamond slide burnishing for improved finishing of structural aluminum elements applied in several industries in order to define the effects of technological parameters of the diamond slide burnishing process on selected properties which would define the product quality.

The burnishing tests were performed on turning/milling center type NL2000SY installation from Mori Seiki controlled in five axes: X, Y, Z, W and C. The burnisher was clamped in machine turret through a special holder. The holder ensures burnishing with elastic pressure and it had stepless pressure force F adjustment. The read-out of pressure force is digital.

The following factors were studied:

a) the kind of pretreatment;
b) the roughness value determined by an amplitude parameter R_a;
c) the number of burnishing passes i;
d) a type of lubricant;
e) the burnishing speed.

The straight turning with the bit tool was applied as the pretreatment. Turning tool gives a beneficial geometrical structure and has a favorable influence on shapes and dimensions of individual surface micro-irregularities. After the turning, we obtain a kinematic geometrical representations of a workpiece and tool movements as well as of cutting edge geometry. The surface roughness before burnishing but after turning was approximately 1 μm. In our experiments we always kept i = 1.

During burnishing a lubricant was applied in the form of a mist of Hysol R Oil from Castrol. The burnishing speed (v = 30 m/min) was constant. Effects of speed on burnishing results have been reported [22, 24, 25]. We have not observed such effects; apparently at our speed detrimental effects of the heat produced are negligible.

We have used the PS/CK (static, factorial, comprehensive) program on which other programs have been built. There is a large variety of combinations of input values.

After burnishing, the geometrical state o the surface layer, the magnitude of material plastic deformation was characterized by measuring a decrease of the burnished shaft radius.

Vickers microhardness h_{Vickers} was determined using a FM 7 tester from Future Tech. Corp., Japan. Microindentations were made using a 10.0 g load.

Metallographic structures were observed with an optical Carl Zeiss Axiovert 100A microscope and a scanning electron microscope (JEOL type JSM-6460LV).

We have used a Hommel Tester T1000 apparatus for determination of the following surface geometry parameters:

– R_a which is the average arithmetic deflection of the roughness profile;

– R_z which is profile height according to 10 points;

– R_{mr} which is the roughness height from the location of 50 % of linear load capacity.

Roughness profilograms were obtained. Surface layer parameters were measured after turning, before and after burnishing.

We have calculated the index of roughness change

$$K_{R_a} = \frac{R_a'}{R_a}, \tag{1}$$

where R_a' is the value before burnishing and R_a afterwards; the same parameters have been used by some of us before [26].

We have also calculated the parameter K_Z of profile deformation defined as

$$K_Z = \frac{\Delta d}{2R_z'}, \tag{2}$$

where Δd is the the value of diameter reduction, R_z' – is value of R_z before burnishing.

Thus, in the case when reduction of the shaft diameter Δd is equal to the dual height of R_z' irregularities, the K_Z indicator is equal to unity.

4. MICROSCOPY AND SPECTRAL ANALYSIS RESULTS

We have determined by scanning electron microscopy the length of elongated Al_2O_3 particles ~17 µm in the A6061 + Al_2O_3 system. In the A390 + SiC composite the average lenght of SiC particles is ~10 µm.

We infer that in our composites strengthening is a result of precipitation from the supersaturated solid solutions of the reinforcing hard particles; this applies to A6061 + Al_2O_3 as well as to A390 + SiC materials. The precipitation can be a consequence of aging – possibly aided by the burnishing treatment.

5. VICKERS HARDNESS

We have determined Vickers microhardness $h_{Vickers}$ for polished sections of specimens at various depths from the burnished surface, thus reaching also into the core of material. The results for A6061 + Al_2O_3 hybrids are presented in Figure 1 (three determinations).

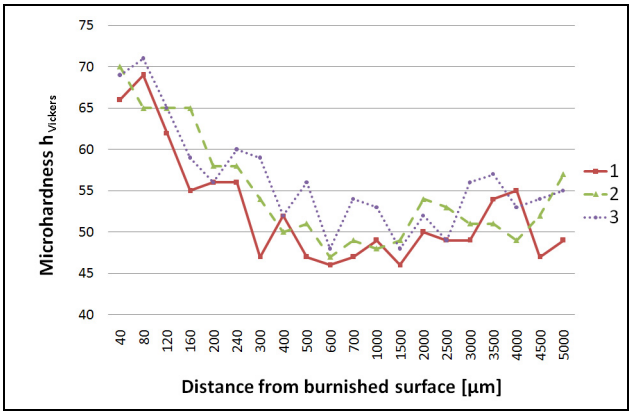

Fig. 1. $h_{Vickers}$ as a function of depth away from the burnished surface for A6061 + Al_2O_3 hybrids (three runs marked 1 – 3)

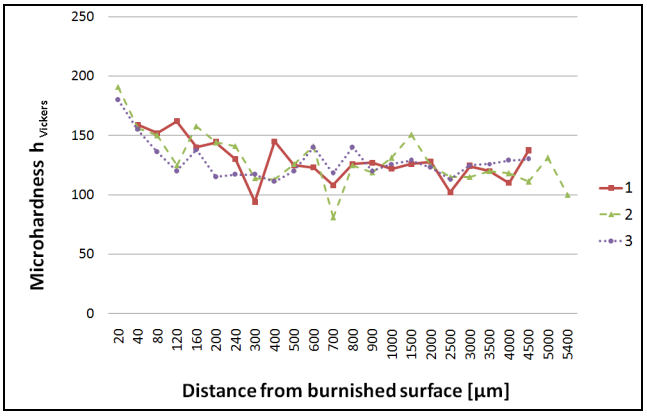

Fig. 2. $h_{Vickers}$ as a function of depth away from the burnished surface for A390 + SiC hybrids (three runs marked 1 – 3)

We find that microhardness at the surface increases approximately 30 % with respect to the core. The thickness of the surface layer amounts to 0.5 mm. That thickness is determined as the depth at which the microhardness becomes equal to that of the sample core.

For the A390 + SiC composite (Figure 2) the microhardness increases even more, up to ~50 % while the surface layer thickness decreases down to 0.3 mm or so.

We recall that in polymers the Vickers hardness is related to the perpendicular groove and top-ridge areas obtained in scratch resistance testing [27]. It remains to be found whether such a relationship exists also in metal matrix composites.

6. SURFACE CHARACTERISTICS

The results of surface roughness measurements and of parameters: R_a, K_{Ra} and K_Z are presented in Tables 1 and 2 and in Figures 3 – 6.

In Fig. 3 we show examples of profilograms of shafts surface roughness after slide burnishing. Fig. 3, a, shows the profilogram for the A6061 + 15 % Al_2O_3 composite and Fig. 3, b, for the A390 + SiC composite. Both profilograms indicate that after burnishing the surface geometry is not a typical predetermined structure – as it was after turning and before burnishing. The surface structure is not random either – like those after abrasive machining such as grinding.

Analysis of our results, in particular the data presented in Tables 1 and 2, shows that our composites have structures intermediate between the typical predetermined ones and random ones. Apparently after diamond slide burnishing of both composites a new surface geometry is formed. However, the K_Z parameter values characterizing deformation irregularities are relatively large. In one case, namely for Sample 8 in Table 1, we have $K_Z = 1.17$. In other cases $K_Z < 1$.

Changes after burnishing in the geometrical structure of the surface are usually assumed to be of two kinds. So called dynamic disturbances have typically a structure with random periodicity. So called tribological disturbances may be caused by several factors, for example by hydrodynamic effect on the tool – machined surface interface or by a lateral plastic flow of the material in the machining area.

Analyzing the surface geometry after burnishing we have to deal with non-decrimental machining. The surface character of aluminum composites (reinforced with hard SiC or Al_2O_3 particles due to diamond slide burnishing) changed after turning from periodic anisotropy to different structures, a result among others of microchipping of hard particles of ceramic as a consequence of the burnishing regime we have applied. Determination of the autocorrelation function as discussed in [28] might be useful in this regard.

We now consider Figures 4 – 6. In Figure 10 we display results for the A6061 + 15 % Al_2O_3 composite after diamond slide burnishing, namely the diagrams of R_a vs. f for several burnishing forces F. We see that an increase of the feed f value results in an increase of the roughness R_a. The minimal value $R_a = 0.15$ µm is obtained for $F = 70.0$ N and $f = 0.02$ mm/rev.

There is no similar minimum for A390 + SiC composite while the R_a values depend significantly on the burnishing force F.

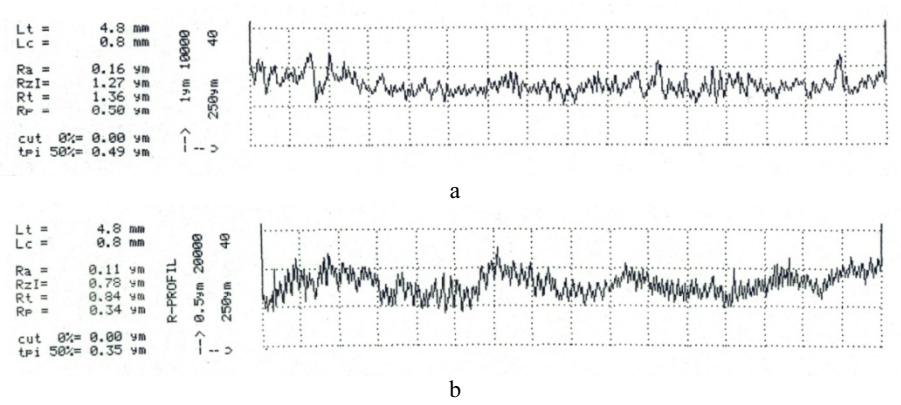

a

b

Fig. 3. Image of burnished surface of A6061 + Al_2O_3 with surface aggregates or clusters of Al_2O_3

Table 1. Test results of the composite A6061 + 15 % Al_2O_3 slide burnishing. Diamond burnisher with nose radio of R = 3.5 mm, v = 30m/min

Test No.	Burnishing force F, N	Feed f, mm/rev	SG parameters after turning			SG parameters after burnishing			K_{Ra}	K_Z
			R_a', µm	R_z', µm	R_{mr}', µm	R_a, µm	R_z, µm	R_{mr}, µm		
1	50	0.02	0.98	4.35	2.4	0.17	1.31	0.80	5.76	0.57
2	50	0.05	0.89	3.82	2.0	0.20	1.31	0.63	4.45	0.79
3	50	0.07	0.95	4.86	2.3	029	1.82	0.80	3.28	0.51
4	70	0.02	0.93	4.22	2.1	0.15	1.14	0.47	6.20	0.83
5	70	0.05	1.03	4.58	2.1	0.19	1.40	0.70	5.42	0.87
6	70	0.07	1.05	4.45	2.1	0.23	1.63	0.77	4.57	0.79
7	90	0.05	1.05	4.26	2.0	0.20	1.50	0.80	5.25	1.17

Table 2. Test results of the composite A390 + 2.5 % SiC slide burnishing. Diamond burnisher with nose radio of R = 3.5 mm, v =30 m/min

Test No.	Burnishing force F, N	Feed f mm/rev	SG parameters after turning			SG parameters after burnishing			K_{Ra}	K_Z
			R_a' µm	R_z' µm	R_{mr}' µm	R_a µm	R_z µm	R_{mr} µm		
1	40	0.02	1.15	4.09	2.00	0.20	1.62	0.47	5.75	0.37
2	40	0.05	1.13	4.08	2.10	0.16	1.18	0.47	7.06	0.86
3	40	0.07	1.08	4.59	2.40	0.31	2.01	0.90	3.48	0.65
4	60	0.02	1.00	4.24	2.30	0.13	0.82	0.37	7.69	0.94
5	60	0.05	0.93	3.62	1.80	0.17	1.12	0.57	5.47	0.69
6	60	0.07	0.89	3.54	1.70	0.14	0.97	0.37	6.36	0.99
7	80	0.02	0.85	4.14	2.00	0.16	1.09	0.47	5.31	0.48
8	80	0.05	0.96	4.95	2.60	0.18	1.61	0.70	5.33	0.40
9	80	0.07	1.03	5.68	2.70	0.17	0.86	0.67	6.06	0.26

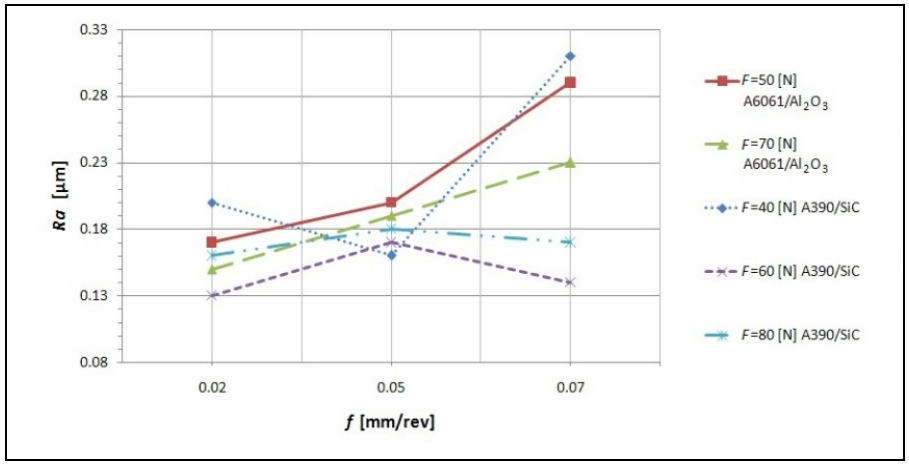

Fig. 4. Relationship R_a–f after diamond slide burnishing of A6061 + 15 % Al_2O_3 and A390 + 2.5 %SiC composites. Diamond burnisher: DCB, nose radius R = 3.5 mm. Standard deviation of R_a is $\delta_{Ra} \approx 0.02$ µm

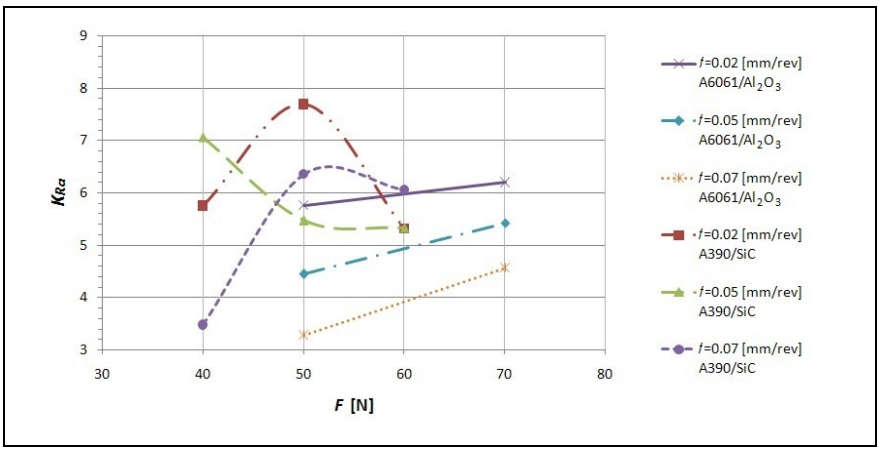

Fig. 5. Relationship $K_{Ra}-F$ after diamond slide burnishing of A6061 + 15 % Al_2O_3 and A390 + 2.5 % SiC composites. Diamond burnisher: DCB, nose radius R = 3.5 mm

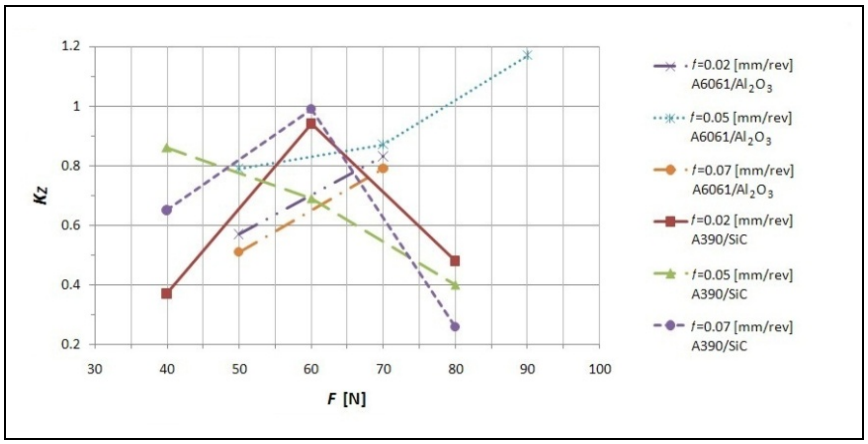

Fig. 6. Relationship K_Z-F after diamond slide burnishing of A6061 + 15 % Al_2O_3 and A390 + 2.5 % SiC composites. Diamond burnisher: DCB, nose radius R = 3.5 mm

Differences between our two composites are also seen in Fig. 5 displaying the K_{Ra} parameter as a function of the force F. While there are some similarities between our two composites, different responses to burnishing are seen, even though the burnishing conditions are similar.

Profile deformation as characterized by the parameter K_Z in Figure 6 depends significantly on the burnishing force F value for the A6061 + 15 % Al_2O_3 composite. Higher value of F gives stronger surface profile deformation. For the A390 + 2.5 % SiC composite, K_Z depends also on F but the diagram $K_Z = K_Z(F)$ shows a local maximum for F = 60 N.

For both composites we find large improvement of characteristic properties caused by the burnishing process:

– R_a for A6061 + 15 % Al_2O_3 goes from approximately 1 μm to 0.15 μm; for A390 + 2.5 % SiC we have the change from approximately 1 μm to 0.13 μm;

– K_{Ra} for A6061 + 15 % Al_2O_3 is = 6.20; for A390 + + 2.5 % SiC it is = 7.69;

– K_Z for A6061 + 15 % Al_2O_3 is = 1.17; for A390 + + 2.5 % SiC it is = 0.99.

7. CONCLUSIONS

We find that burnishing provides a capability to improve significantly the surface topography in both A6061 + 15 % Al_2O_3 and A390 + 2.5 % SiC composites. Especially the surface roughness R_a increases significantly so that K_{Ra} goes up to 6.20 for A6061 + 15 % Al_2O_3 bars and to 7.69 for A390 + 2.5 % SiC bars. The parameter R_{mr} decreases from 2.1 to 0.47 for A6061 + 15 % Al_2O_3 and from 2.30 to 0.37 for A390 + 2.5 % SiC MMCs. In case of Al_2O_3 containing composites the increase of K_{Ra} is not as large as for the case of SiC containing composites since Al_2O_3 particles disintegrate as a consequence of the burnishing process.

Surface strengthening defined as increase of microhardness due to burnishing ((microhardness of the surface/microhardness of the core layer) × 100 %) after burnishing is for A6061 + 15 % Al_2O_3 about 30 % while for A390 + 2.5 % SiC the respective value is about 50 %. Thus better wear resistance of burnished surfaces has been achieved.

As already noted, both MMCs we have investigated are frequently used in automotive and aeronautic components. Burnishing does improve the surface topography – important in applications that require good tribological properties. However, introduction of a reinforcement can be a two-edged sword. Voids might be formed from Al_2O_3 clusters desintegrating near the surfaces of the components. Under dynamic loads and unfavorable service conditions fatigue fracture might originate from the voids. More generally, a number of other techniques is available such as galvanization [29] or

heat treatment. Nitriding is another technique that can be used [26].

Acknowledgments

We thank the Materials Engineering and Sintering Centre team, IAMT, for SEM and electron probe micro–analyzes (EPMAs) as well as for microhardness tests.

REFERENCES

1. **Kopczynska, A., Ehrenstein, G. W.** Polymeric Surfaces and Their True Surface Tension in Solids and Melts *Journal Materials Education* 29 2007: pp. 325 – 340.
2. **Desai, R. C., Kapral, R.** Dynamics of Self-organized and Self-assembled Structures. Cambridge University Press, Cambridge – New York, 2009. http://dx.doi.org/10.1017/CBO9780511609725
3. **Świrad, S.** Kompozyty diamentowe – materiały supertwarde do obróbki nagniataniem (Diamond Composites – Superhard Materials for Diamond Burnishing) *Zeszyty Naukowe Politechniki Rzeszowskiej Mechanika* z. 66. Rzeszów, 2006 (in Polish).
4. **Korzyński, M., Lubas, J., Swirad, S., Dubek, K.** Surface Layer Characteristic due to Slide Diamond Burnishing with a Cylindrical-ended Tool *Journal of Materials Processing Technology* 211 2011: pp. 84 – 94.
5. **Polowski, W., Bednarski, P.** Badania technologiczne procesu nagniatania ślizgowego przy użyciu nagniataków diamentowych wykonanych na bazie kompozytów diamentowych produkowanych w IZTW (A Technological Study of Slide Burnishing Process Using Tools Made from Diamond Composites Produced in IAMT) *Prace IZTW Seria Sprawozdania*, Kraków, 2010 (in Polish).
6. **Przybylski, W., Zieliński, J.,** Obróbka wykańczająca stopów aluminium przez nagniatanie ślizgowe (Finishing Treatment of Aluminium Alloys by Slide Burnishing) *Materiały z IX Konferencji Naukowej Technologia Obróbki przez Nagniatanie TON'05* Gdańsk, 13 – 14. 10. 2005 (in Polish).
7. **Lopez de Lacalle, L. N., Lamikiz, A., Munoa, J., Sanchez, J. A.** Quality Improvement of Ball-end Milled Sculptured Surfaces by Ball Burnishing *International Journal of Machine Tools & Manufacture* 45 2005: pp. 1659 – 1668.
8. **Świrad, S.** Influence of Parameters of Sliding Burnishing with Cylindrical Elements on Surface Roughness *The Fifth International Conference on Mechanics* 2006: pp. 223 – 228.
9. **Przybylski, W.** Technologia obróbki nagniataniem (Burnishing Technology) *WNT*, Warszawa, 1987 (in Polish).
10. **Ogburn, F.** Roll to the Finish *Cutting Tools Engineering* 6 2001: pp. 50 – 54.
11. **Hassan, A. M., Momani, A. M. S.** Further Improvements in Some Properties of Shot Peened Components Using the Burnishing Process *International Journal of Machine Tools & Manufacture* 40 2000: pp. 1775 – 1786.
12. **Pawlus, P., Dzierwa, A.** Functional Importance of Surface Topography Parameters *The Sixth International Conference on Mechanics* 229 – 237 2008.
13. **Kanapenas, R.** Laser Hardening of Tool Steel of Various Grades *Materials Science* (*Medžiagotyra*) 7 2001: pp. 10 – 14.
14. **Tian, Y., Shin, Y. C.** Laser Assisted Burnishing of Metals *International Journal of Machine Tools & Manufacture* 47 2007: pp. 14 – 22. http://dx.doi.org/10.1016/j.ijmachtools.2006.03.002
15. **Yan, B. H., Wang, C. Ch., Chow, H. M., Lin, Y. Ch.** Feasibility Study of Rotary Electrical Discharge Machining with Ball Burnishing for Al2O3/6061 Al Composite *International Journal of Machine Tools & Manufacture* 40 2000: pp. 1403 – 1421. http://dx.doi.org/10.1016/S0890-6955(00)00005-5
16. **Davis, J. R.** ASM Specialty Handbook: Aluminum and Aluminum Alloys *ASM International* 1993.
17. **Duszczyk, J., Bialo, D.** Friction and Wear of P/M Al–20SiAl_2O_3 Composites in Kerosene *Journal of Materials Science* 28 1993: pp. 193 – 202.
18. **El-Tayeb, N. S. M., Low, K. O., Brevern, P. V.** Influence of Roller Burnishing Contact Width and Burnishing Orientation on Surface Quality and Tribological Behaviour of Aluminum 6061 *Journal of Materials Processing Technology* 186 2007: pp. 272 – 278. http://dx.doi.org/10.1016/j.jmatprotec.2006.12.044
19. **Biało, D.** Zużycie tribologiczne kompozytów na osnowie stopów aluminium otrzymanych z proszków (Tribological Wear of Aluminium Matrix Composites Based on Powders) *Prace Naukowe – Mechanika* Zeszyt nr 192 Oficyna Wydawnicza Politechniki Warszawskiej Warszawa, 2002 (in Polish).
20. **Ye, H.** An Overview of the Development of Al.-Si-Alloy Based Material for Engine Applications *Journal of Materials Engineering and Performance* 12 (3) 2003: pp. 288 – 297. http://dx.doi.org/10.1361/105994903770343132
21. **Czechowski, K., Polowski, W., Wronska, I., Wszołek, J.** Nagniatanie ślizgowe jako metoda obróbki wykończeniowej powierzchni (Slide Burnishing as a Machining Method of Surface Finishing) *Projektowanie i Konstrukcje Inżynierskie* Wrzesień, 2009: pp. 21 – 27 (in Polish).
22. **Jaworska, L.** Wysokociśnieniowe spiekanie proszków diamentowych (High Pressure Sintering of Diamond Powders) *Prace Instytutu Obróbki Skrawaniem* Seria „Zeszyty Naukowe" No 82, Kraków, 2002 (in Polish).
23. **Polowski, W., Stós, J., Bednarski, P., Czechowski, K., Wszołek, J.** Nagniatanie ślizgowe narzędziami diamentowymi (Slide Burnishing by Means of Diamond Tools) *Mechanik* 12 2010: pp. 965 – 967 (in Polish).
24. **Polowski, W., Bednarski, P., Toboła, D.** Obróbka wykończeniowa narzędziami diamentowymi do nagniatania ślizgowego (Finish Machining with Diamond Slide Burnishing Tools) *Postępy nauki i techniki* 6 2011: pp. 40 – 49. Oddział SIMP w Lublinie, 2011 (in Polish).
25. **Korzyński, M.** Nagniatanie ślizgowe (Slide burnishing) *WNT* Warszawa, 2007 (in Polish).
26. **Brostow, W., Czechowski, K., Polowski, K., Rusek, P., Toboła, D., Wronska, I.** Slide Diamond Burnishing of Tool Steel with Adhesive Coatings and Diffusion Layers *Materials Research Innovations* 17 2013 (to be published).
27. **Brostow, W., Chonkaew, W., Rapoport, L., Soifer, Y., Verdyan, A.** Grooves in Scratch Testing *Journal of Materials Research* 22 2007: pp. 2483 – 2487.
28. **Oczoś, K., Liubimov, V.** Struktura geometryczna powierzchni (Geometrical Structure of Surfaces) Oficyna Wydawnicza Politechniki Rzeszowskiej, Rzeszów, 2003 (in Polish).
29. **Pociene, A., Dudonis, J., Pocius, M., Meskauskas, A.** The Influence of Steel Substrate Surface Relief on Fe-Zn Alloy Coating in Hot-dip Galvanization *Materials Science* (*Medžiagotyra*) 16 2010: pp. 302 – 306.